Materials Analysis Using Confocal Raman Microscopy

Chris Sammon, Sohail Hajatdoost[1], Peter Eaton, Carine Mura and Jack Yarwood*

Sheffield Hallam University, Materials Research Institute, City Campus,
Howard Street, Sheffield S1 1WB, UK
[1]British Steel plc, Trostre Works, Llanelli, Dyfed, SA14 9SD, UK

ABSTRACT

The recent development of Raman microscopes with high optical throughput and very sensitive CCD cameras has led to Raman spectroscopy again competing effectively with FTIR methods for materials analysis. Modern Raman instruments, designed to operate confocally without serious alignment or energy trade-off problems, allow depth profiling of optically transparent polymers and polymer matrices to be routinely obtained with a spatial resolution of 1-2 μm. The use of such an instrument is illustrated by describing recent work on polymeric material problems including,

1 The distribution and redistribution of small molecules in polymeric matrices.
2 The monitoring of adhesion primer diffusion at a polymer/silica interface.
3 The determination of the extent of interdiffusion and interaction at a polymer/polymer interface.
4 A comparison of confocal and micotoming approaches to polymer laminate analysis.

The range of possible applications is increasing rapidly. It is clear that Raman microscopy will become a very important tool for future materials analysis, both in the polymer area and many other areas.

 CCC 1022-1360/99/$ 17.50+.50/0

1 INTRODUCTION

Advances in source, detector, filter and computer technologies[1-4] have led to the rebirth of Raman spectroscopy. In particular, the coupling of a high quality optical microscope and a high throughput Raman spectrometer have significantly extended our ability to do in-situ measurements on a wide variety of materials where a combination of high sensitivity and high spectral and spatial resolution is required[5-20]. It is now common to find such measurements being made in an industrial context[6-8], including remote sensing. An extremely wide range of material types has also been studied, covering areas such as mineralogy, biochemistry, polymer science, medicine and electrode processes[5-11].

Sensitivity levels[12-15] are now comparable with those of infrared spectroscopy, certainly for bands with a high Raman cross-section. Because of the well established empirical complementarity of transition dipole and transition polarisability functions, Raman microscopy is often feasible when infrared spectroscopy is not. Furthermore, there are several well known advantages (Table 1) of Raman microscopy compared with infrared microscopy. The principal one, in this context, is the shorter wavelength and consequent implication for spatial resolution. With modern equipment a spatial resolution of 1-2 μm may be achieved in any of the X, Y or Z directions. This allows the optical microscope to be set up in confocal mode[3,12,13,15,18-20] and to do non-destructive and rather elegant depth profiling; something which cannot be achieved with infrared microscopy without microtoming the sample.

2 Experimental

Figure 1 shows the principle of Raman microscopy[16,20] as realised in the Renishaw 2000 instrument used for this work. A stigmatic single spectrograph was attached to an Olympus BH2 microscope. The instrument was then set up in confocal mode with a X100 short working-length objective (NA = 0.95). The slit width was about 15

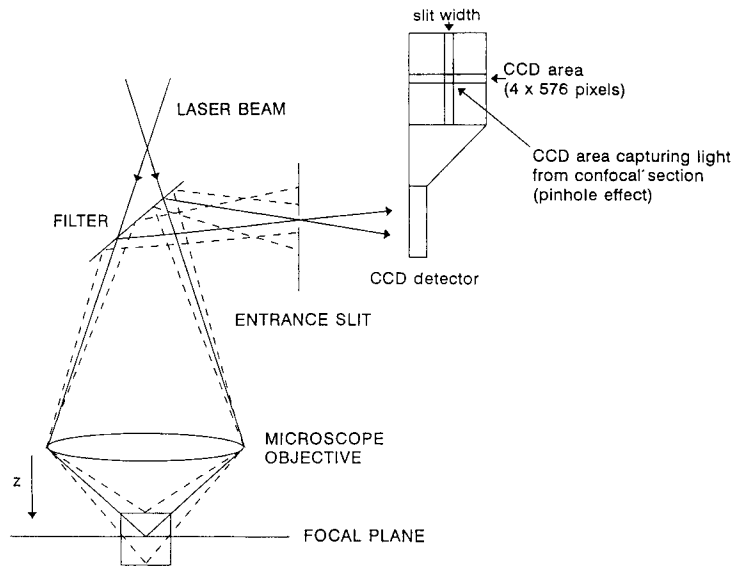

Fig 1 Schematic diagram of the principle of confocal Raman microscopy using a CCD camera. (Reproduced by permission from Appl. Spectroscopy 50 558 (1996))

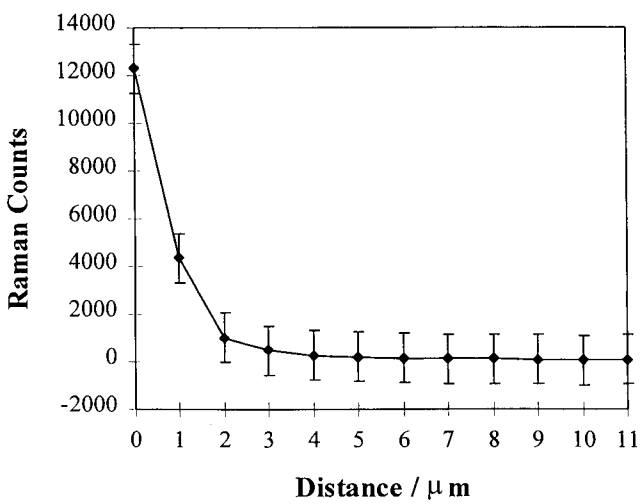

Fig 2 The microscope confocal profile for X100 objective obtained using the silicon Raman band at 520 cm^{-1}.

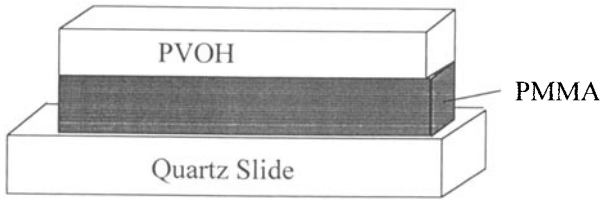

Fig 3 Schematic of PVOH / PMMA laminate cast onto a quartz slide

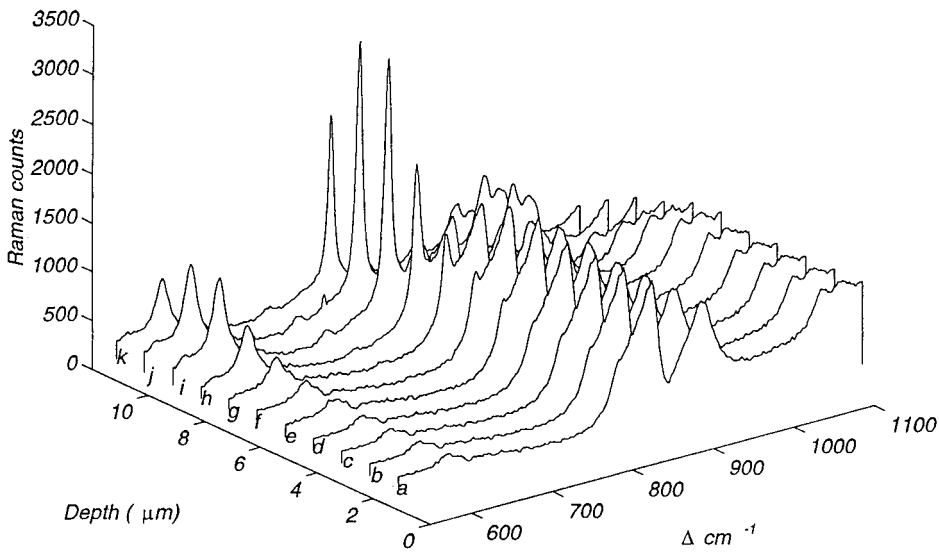

Fig 4 Raman microscopic spectra of the laminate shown in figure 3 as a function of depth into the material. Bands at 813 cm^{-1} and 610 cm^{-1} arise as the laser focusing depth increased. (Reproduced by permission from Appl. Spectroscopy 50 558 (1996))

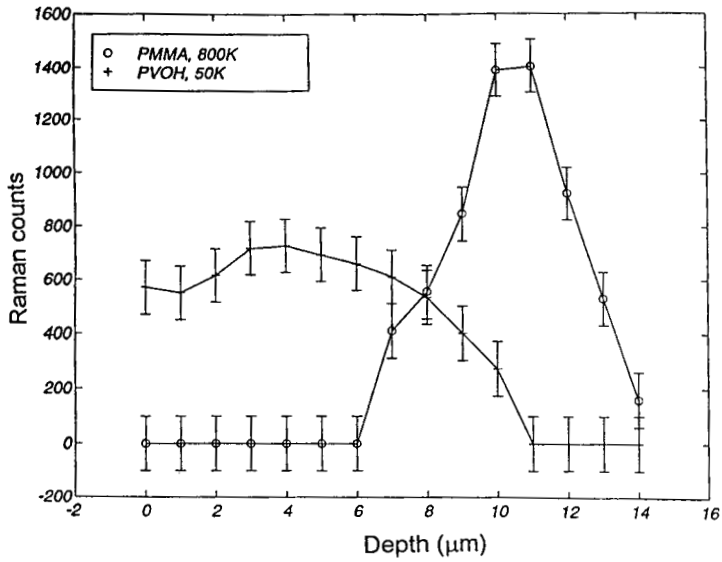

Fig 5 Plot of Raman counts as a function of depth for a PMMA / PVOH laminate as shown schematically in Fig 3. The data are taken from Fig 4. The physically measured interface between the two polymers is at 9.5 ± 0.5 μm below the surface. (Reproduced by permission from Appl. Spectroscopy 50 558 (1996))

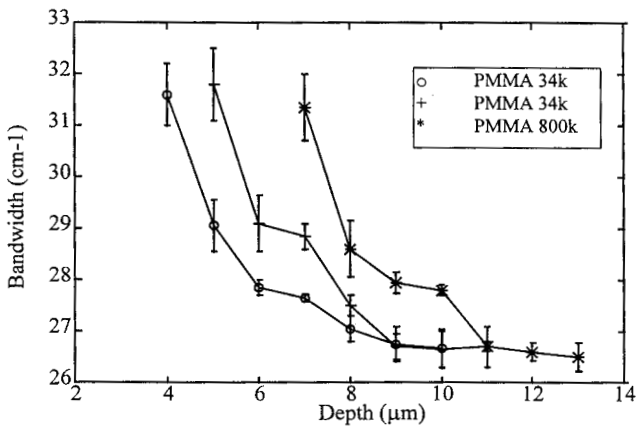

Fig 6 Variation of band width of the ν(C=O) band of PMMA as a function of depth into a PVOH / PMMA laminate (Reproduced by permission from Appl. Spectroscopy 50 558 (1996))

microns and a CCD area of 4 x 576 pixels was used. The long axis, 576 pixels, defines the spectral dimension and the short axis describes the height of the image. This arrangement of CCD camera and the spectrometer slit mechanism acts as a pin-hole for the blocking of out-of-focus signals which arise from above and below the sample plane. The depth of resolution of the confocal arrangement achieved this way was checked by using a silicon sample as a reference material. In this experiment (Figure 2) the focus of the laser was step-wise (1 micron) scanned away from the silicon surface and the signal intensity of the vibrational band at 520 cm^{-1} was recorded. As Figure 2 shows, the confocal profile had a full half width of between 1.5 and 2 cm^{-1} and it is clear that about 90% of the scattered light is contributed from about 2.5 microns below and above the plane of focus. This allows the exploration of interfacial phenomena in optically transparent media, as described below.

CONFOCAL RAMAN MICROSCOPY

VIBRATIONAL SPECTROSCOPY AT HIGH SPATIAL RESOLUTION

- SPATIAL RESOLUTION 1 - 2 μm, XY +Z MAPPING AND IMAGING
- COMPLEMENTARITY WITH IR MICROSCOPY
- *IN SITU* DEPTH PROFILING MEASUREMENTS IN REAL TIME
- HIGH SENSITIVITY ON ~MONOLAYER SCALE (UN-ENHANCED)
- OPPORTUNITIES FOR 'ENHANCEMENT' VIA SERS, RRS, SERRS, ETC.

3 RESULTS AND DISCUSSION

3.1 The Buried Interface

Investigations of phenomena which occur at the interface between two polymers [figure 3] is of considerable practical importance in the context of interdiffusion, interactions, and adhesions at such polymer interfaces. Whilst Raman methods cannot probe the near interface (i.e. the first few nm either side of the physical barrier) it is possible to detect, on a micron scale, the effects of interpenetration and molecular interactions, especially those processes associated with the extrusion, casting or

annealing processes[20] which are necessary to produce functional laminate structures. We have shown[20] that, for example, the interactions and interdiffusion of PVOH and PMMA can easily be detected (Figures 4-6). In Figure 4 we displayed the Raman spectra obtained in confocal mode as a function of depth into a PVOH (4.5 μm)/ PMMA(9.5 μm) laminate. These demonstrate (see Figure 5) that the PMMA and the PVOH have mixed, probably during the casting process (which involves annealing at 70°C to remove the solvent) and that PMMA is detected at about 4 μm above the supposed physical interface between the two polymers. There is, however, a 2 μm displacement[20] of the confocal profile due to a refractive index change at the polymer surface, but it is clear that strong, hydrogen bonding-interactions, as measured by the width of the ν(CO) band of the PMMA occur between the different chemical groups on the two polymer chains (Figure 6). This demonstrates that PMMA is dissolved in the PVOH matrix as much as 2 μm above the physical interface.

More recently[21] we have compared the interfacial chemical structure of extruded PET using both confocal microscopy (Z-direction) and using a laterally microtomed section (in the X-Y mode). The material was a commercially available grade Melinex© 850 film, either 20 or 30 μm in thickness. This film consisted of a co-extruded laminate, with a thin amorphous copolyester on a thicker semi-crystalline base. The films were biaxially drawn, thermally annealed and cut into the desired shape. Two samples were prepared for each film, one with the amorphous side up and the other with the semi-crystalline side up. For the sideways on-depth profile, the clean edge was cut using a scalpel and the film was supported on a small piece of plasticine so that the clean edge was facing the Raman microscopy. A nominal spatial resolution of 1 μm was used both for the confocal mode and for the X-Y mapping of the sideways on section. The results are shown in Figures 7 and 8. Since the two components of the laminate are expected to have different crystallinities a method is needed to distinguish such differences using Raman spectroscopy. In Figure 7 we demonstrate that the PET carbonyl band at $\sim 1720\ cm^{-1}$ has a width which depends on the percentage of amorphous material in a semi crystalline PET (Figure 7A), Figure 7B shows the change of width measured across the interface for a real 20 micron

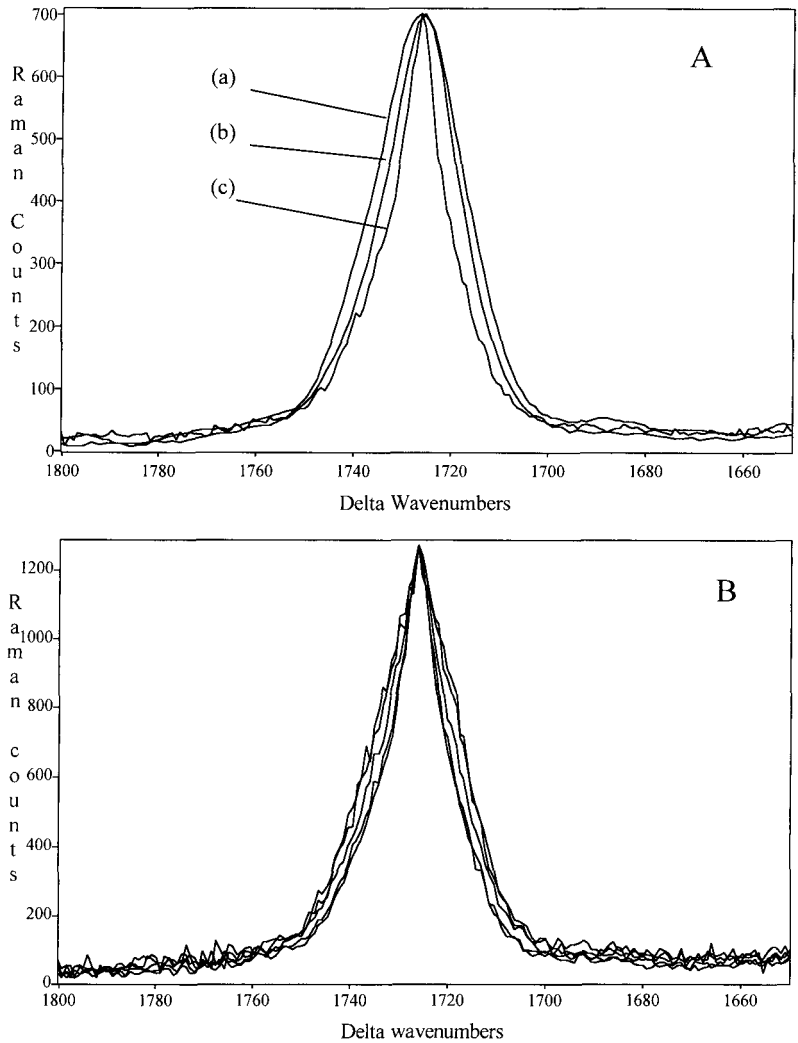

Figure 7 (A) The ν(C=O) of 100 % amorphous (a), 25 % (b) and 50 % (c) crystalline PET.
(B) The changes in width of the carbonyl band at the interface of a 20 μm Melinex© 850 laminate, measured using confocal Raman microscopy.

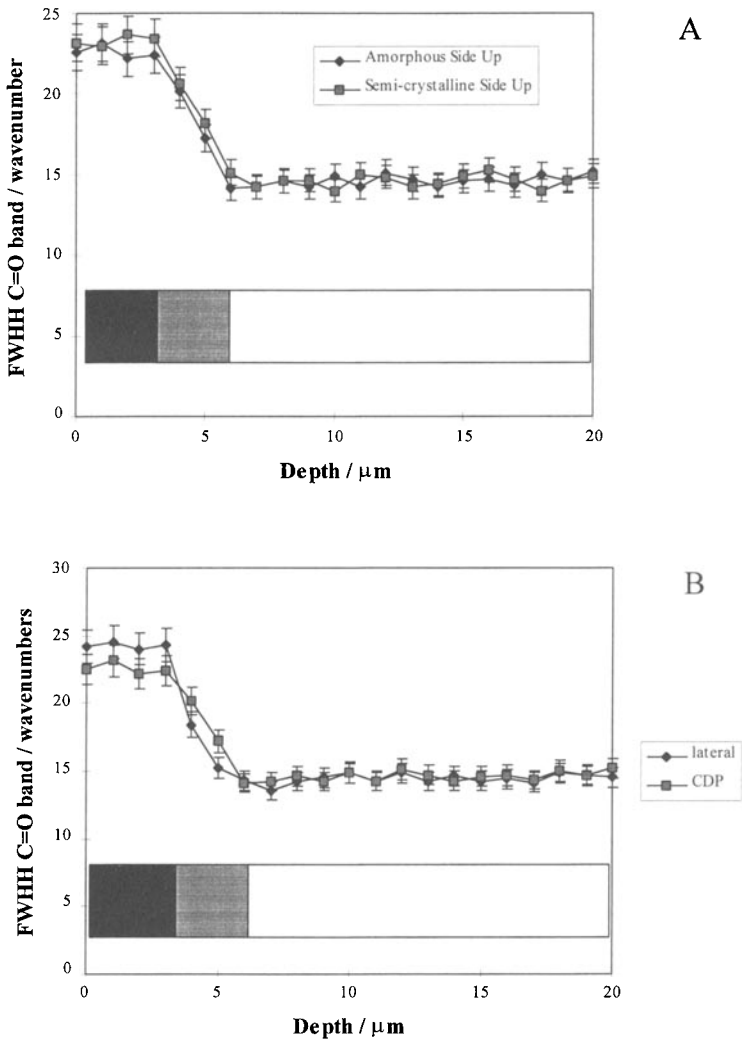

Figure 8 (A) The ν(C=O) band width as a function of depth (in confocal mode) for a 30 μm PET laminate
(B) Comparison of the interfacial gradients measured for a 20 μm PET laminate for the two depth profile experiments

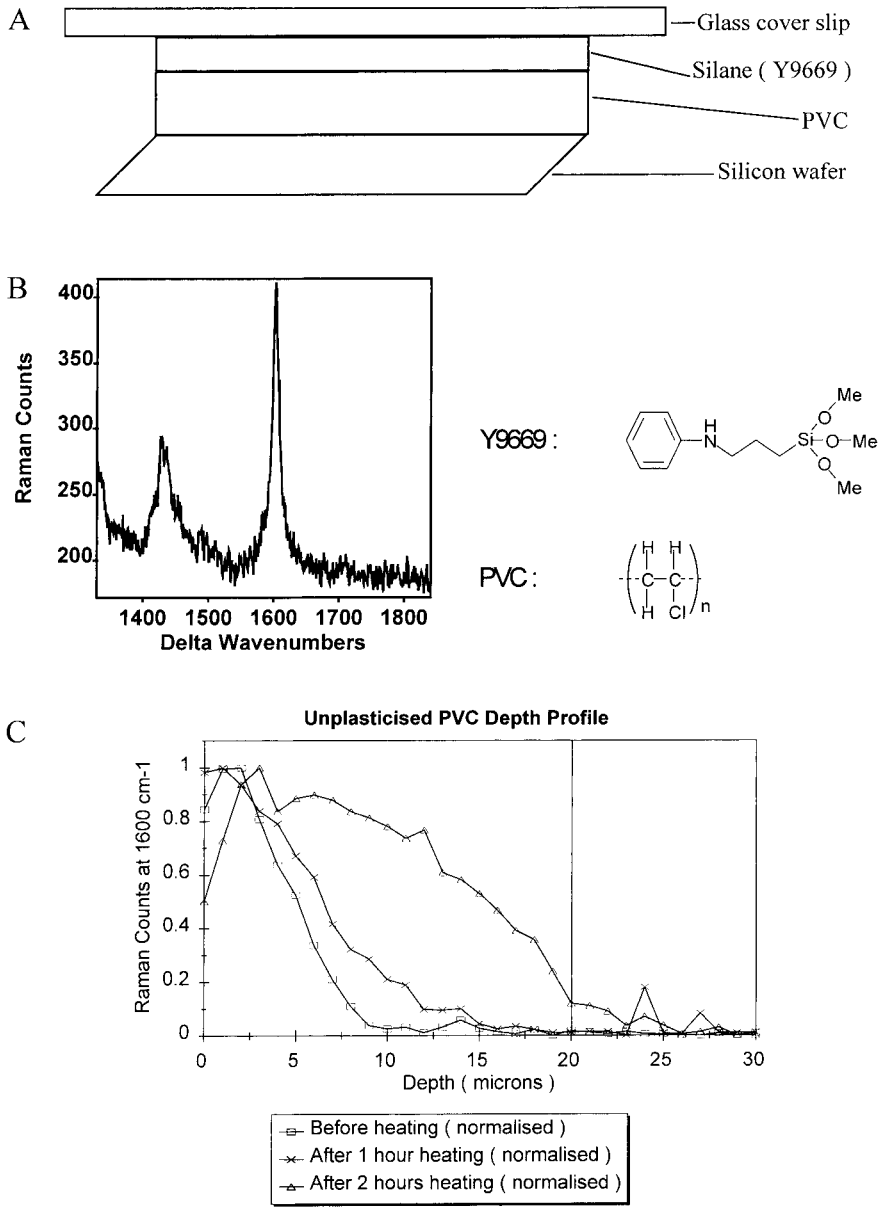

Fig 9 (A) The silane / PVC matrix structure (B) the 1602 cm^{-1} band of Y9669 (B) The silane distribution with depth into PVC as a function of annealing temperature

Melinex© 850 laminate. In Figure 8 we show the change of Raman ν(CO) band half width as a function of depth into a 30 μm Melinex© 850 film and the associated physical structure. In Figure 8B we compare the confocal depth profile with the lateral (X-Y profile) along the edge of a 20 micron Melinex© 850 film. Although the profile is somewhat 'sharper' in 'lateral' than in 'confocal' mode the data are semi-quantitatively the same. We conclude that the interfacial region with its corresponding crystallinity gradient[26] (probably caused by trans-esterfication occurring as the two molten polymers come into contact with each other) may be studied using confocal microscopy.

3.2 Diffusion/redistribution processes

Other applications of the use of a confocal Raman microscope to study polymeric materials of commercial interest include the study of the distribution and/or redistribution processes as a function of depth into a transparent matrix. For example, Figure 9 shows the redistribution from the surface, of a silane adhesive primer (Y9669) in a PVC film as a function of annealing time (70^{o}C)[27]. These measurements were made by focusing to successive depths (with a 1 micron precision, at room temperature) following the annealing process and integrating the ring breathing band at 1602 cm^{-1} (Figure 9B). As may be observed, the diffusion of the silane towards the polymer interface is significantly promoted (as expected) by heating the polymer to near the glass transition temperature. In the industrial situation, glass polymer laminates are formed at much higher temperatures ensuring the high quality adhesion is achieved. These measurements demonstrate why heating is required, especially for the unplasticised polymer. It should be noted that the data in Figure 9C may be deconvoluted [27] from the confocal profile of the microscope (Figure 2) to give an accurate picture of the widening silane distributions as a function of heating.

Finally, we have demonstrated[28] the ability to study the distribution and / or redistribution of small molecules (in particular plasticiser additives) as a function of ambient conditions in important commercial situations. Figure 10 shows an example

Fluorofolpet (PA3)

(A)

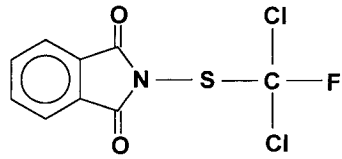

(B)

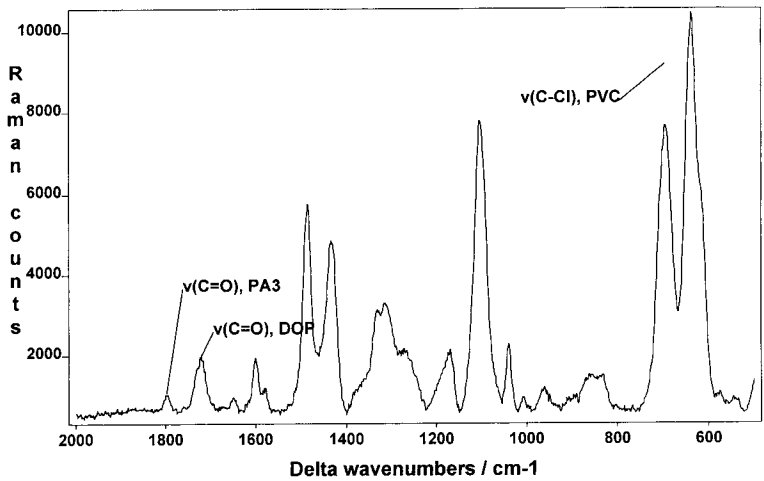

(C)

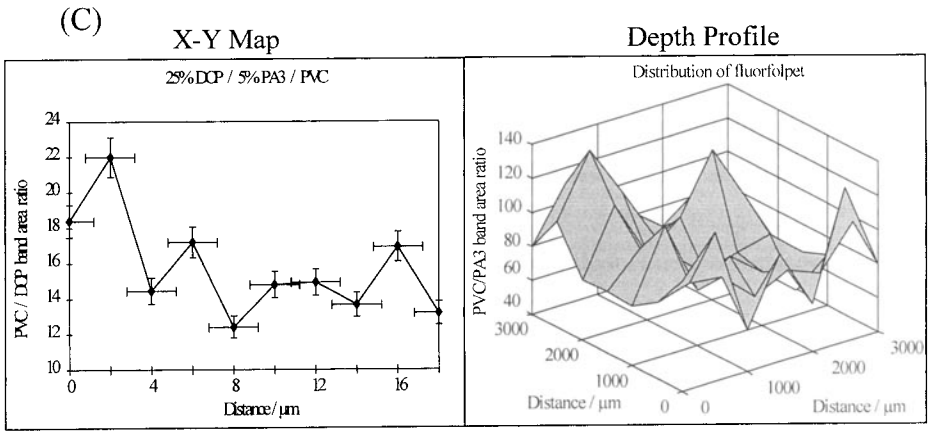

Fig 10 (A) The structure of Fluorofolpet (PA3)
(B) The Raman spectrum of biocide (PA3) and plasticiser (DOP) in a PVC matrix
(C) Map of XY and Z concentrations in the PVC matrix

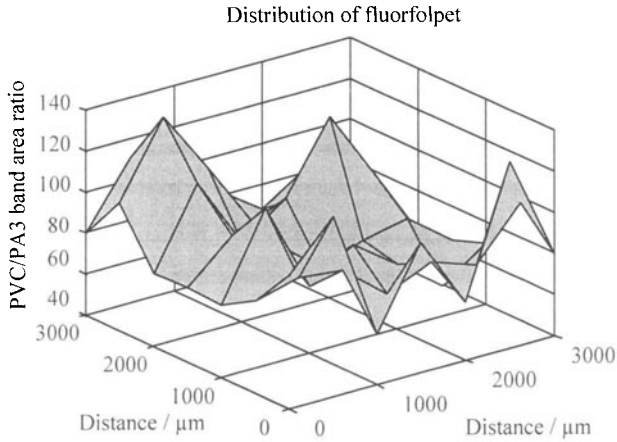

Map 1 86 ± 20
Map 2 77 ± 12
Map 3 82 ± 17

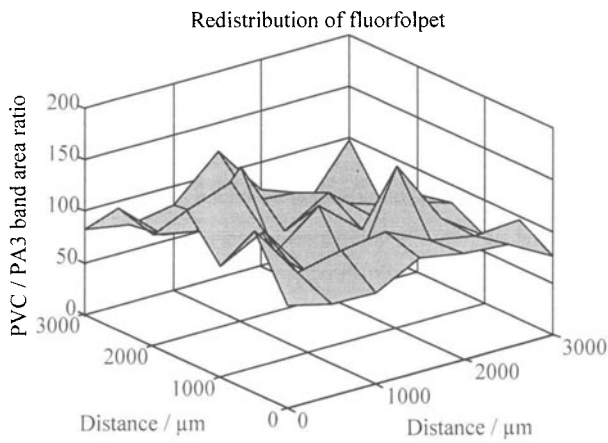

Map 1 119 ± 57
Map 2 108 ± 53
Map 3 97 ± 26

Fig 11 Comparison of maps and statistical distribution averaged (PVC/PA3 band ratios) of PA3 in PVC before and after leaching in water for 5 hours at room temperature

of mapping (X-Y) and depth profiling (Z) the concentration of a biocide Fluorfolpet in a cast film of PVC. The statistical data (Figure 10C) show clearly that the distribution of biocide is homogeneous on a macroscopic scale, but heterogeneous on a microscopic (sub micron) scale. In order to monitor the possible leaching of biocide the polymer matrix was soaked in water for several hours at 25°C. Figure 11 shows that indeed significant leaching of a biocide occurs. However, there is no evidence of accumulation near the polymer surface. These results have been confirmed using FTIR measurements and dynamic leaching experiments using a rotating disc apparatus.

4 CONCLUSION

It is clear that the Raman microscope is an important future tool in materials science. The technique will contribute, along with others such as AFM / STM, SEM, FTIR etc., in a complementary way to the detailed understanding of material properties and processes. Instrument manufacturers can look forward to a healthy future.

ACKNOWLEDGMENT

We thank EPSRC (for instrument purchase) and Zeneca, Pilkington and ICI (Wilton) for additional financial support. Detailed discussions with Dr N Everall, Mr J Chalmers, Mr R Swart, Dr P Holmes and Dr D Hodge are also gratefully acknowledged.

REFERENCES

1 D N Batchelder, C Cheng and G D Pitt, Advanced Materials, 3, 566 (1991); Measurements in Science and Technology, 3, 561(1992).

2 G J Puppels, W Colier, J H F Olminkof, C Otto, F F M Demul and J Greve, J. Raman Spectrosc., 22, 217(1991).

3 P J Treado and M J Morris, Infrared and Raman Spectroscopic Imaging, Applied Spectrosc. Rev., 29, 71-108(1994).

4 B Schrader, Micromethods in Infrared and Raman Spectroscopy, Fresenius J. Anal. Chem., 337, 824(1990); B Schrader, G Baranovic, G Keller and J Sawatzki, Fresenius J. Anal. Chem., 349, 4(1994).

5 R A Dluhy, S M Stevens, S M Widyatai and A D Williams, Spectrochimica Acta 51 1413(1995).

6 J Andrews, Spectroscopy Europe, 7, 8(1995).

7 I R Lewis and P R Griffiths, Appl. Spectros., 50,12A(1996).

8 Industrial Analysis with Vibrational Spectroscopy, J. M Chalmers and G Dent, Royal Soc. Chemistry London (1997).

9 J Berbillat, P Dhamelincourt, M Delhaye and E da Silva, J. Raman Spectroscopy, 25, 3(1994); Spectros. Eur., 5 16(1993).

10 P V Huong, Vibrational Spectroscopy, 11, 17(1996).

11 N Everall, H Owen and J Slater, Appl. Spectroscopy, 49, 610 (1995).

12 K J P Williams, G D Pitt, B J E Smith, A Whitley, D N Batchelder and I P Hayward, J. Raman Spectroscopy, 25, 131(1994).

13 D J Gardiner and M Bowden, Microscopy and Analysis, Nov. 1990, p, 27 (and references therein).

14 A.Govil, D M Pallister, L-H Chen and M D Morris, Applied Spectroscopy, 45, 1604(1991), ibid, 47, 75(1993).

15 R Tabaksblat, R J Meier and B J Kip, Applied Spectroscopy, 46, 60(1992).

16 K J P Williams, G D Pitt, D N Batchelder and B J Kip, Applied Spectrosc., 48, 232(1994).

17 A Garton, D N Batchelder and C Cheng, Applied Spectrosc., 47, 922(1993).

18 T Kasteleiner, R M Swart, D J Hodge and J Yarwood, J. Raman Spectros., 27, 695(1996).

19 S Hajatdoost, R Banga, R Evans, T Kasteleiner and J Yarwood, Spectrosc., Europe, 8, (1996).

20 S Hajatdoost, M Olsthoorn and J Yarwood, Appl. Spectrosc. 50, 558(1996); ibid; 51, 1784(1997).

21 C Sammon, PhD Thesis, Sheffield Hallam University (1997)

22 A J Melveger, J. Polym. Sci. (A2), 10, 317,(1972).

23 J M Chalmers, L Croot, G J Eaves, N Everall, W F Gaskin, J Lumsden and N Moore, Spectrosc.Int. J., 8, 13(1990).

24 N Everall, P Taylor, J M Chalmers, D Mackerron, R Ferwerda and J van der Maas, Polymer, 33, 15, 3184(1994).

25 N Everall, K Davis, H Owen, M J Pelletier and J Slater, Appl. Spec. 50, 386(1996).

26 E Andersson and H G Zachman, Coll. Polym. Sci., 272, 1352(1994).

27 P Eaton, PhD Thesis, Sheffield Hallam University (1998).

28 C Mura, PhD Thesis, Sheffield Hallam University (1998).